Saturation spectroscopy and electronic-state lifetimes in a magnetic field in InAs/$Al_xGa_{1-x}Sb$ single quantum wells

S. K. Singh and B. D. McCombe
Department of Physics, State University of New York at Buffalo, Buffalo, New York 14260

J. Kono
Hansen Experimental Physics Laboratory, Stanford University, Stanford, California 94305

S. J. Allen, Jr.
Center for Terahertz Science and Technology, University of California at Santa Barbara, Santa Barbara, California 93106

I. Lo
National Sun Yat-Sen University, Kaohsiung, Taiwan, Republic of China

W. C. Mitchel and C. E. Stutz
Wright Laboratory, Wright-Patterson Air Force Base, Dayton, Ohio 45433

(Received 7 May 1998)

Saturation spectroscopy of electronic states in InAs/$Al_xGa_{1-x}Sb$ single-quantum-well structures has been carried out with the UCSB free-electron laser. An effective Landau-level lifetime is extracted from the cyclotron-resonance (CR) saturation results on a semiconducting sample ($x=0.5$) with the help of an *n*-level rate equation model. The effective lifetime shows strong oscillations (greater than an order of magnitude) with laser frequency with minima shifted to higher frequencies than given by the simple parabolic magnetophonon resonance condition due to large nonparabolicity in the InAs conduction band. Similar saturation studies of two lines (the *X* line and CR) in a ''semimetallic'' sample ($x=0.1$) show markedly different effective lifetimes, demonstrating that the two lines are of different origin. [S0163-1829(98)04336-7]

I. INTRODUCTION

The understanding of the dynamical relaxation processes of hot carriers in bulk and confined semiconductors is of interest from both scientific and technological points of view. These relaxation processes contain important information about the interaction between carriers and lattice, between carriers and impurities or traps, and among carriers themselves. Saturation spectroscopy can be used to probe these relaxation processes. In principle, by measuring the intensity dependence of the resonance absorption one can extract the carrier lifetime in the excited state. This technique has been used to determine the lifetime of confinement states in multiple-quantum-well structures,[1,2] shallow hydrogenic impurity states in bulk[3] and quasi-two-dimensional semiconductors,[4] and Landau levels in bulk GaAs,[3,5] InSb,[3] and in GaAs/Al_xGa_{1-x}As single heterostructures[6,7] and multiple quantum wells.[4,8] Saturation spectroscopy has also been used to study the effective Landau-level (LL) lifetime as a function of electron density. The effective lifetime was found to depend inversely on the electron concentration both in bulk GaAs (Refs. 1 and 5) and GaAs/Al_xGa_{1-x}As single heterostructures.[7]

The interaction between electrons and LO phonons has been studied for many years.[9] This interaction is effectively screened at high electron densities at low temperatures and for low-intensity far-infrared radiation.[10] However, it has been shown theoretically in zero magnetic field[11] and in a magnetic field[12] that at high electron temperatures the dynamic screening does not depend strongly on the electron density for a two-dimensional (2D) electron gas. This is supported by various experiments.[13,14] For example, Barnes *et al.*[13] showed that the magnitude of the magnetophonon contribution to the cyclotron resonance (CR) linewidth is independent of the carrier density at high temperatures in GaAs/Al_xGa_{1-x}As heterostructures. At high laser powers near CR, higher LL's can be significantly populated; this situation mimics a high electron temperature. Therefore, at high laser powers it is possible to observe substantial effects of electron–LO-phonon interaction even in samples having a high electron density.

Magnetophonon resonances (MPRs) are typically observed as oscillations in the transverse and longitudinal magnetoresistance when the separation between two LL's equals the LO-phonon energy.[15] MPRs have also been observed as oscillations in the linewidth of CR at high temperatures.[13] Recently, Vaughan *et al.*[16] have observed an oscillatory behavior of an effective LL lifetime as a function of frequency (between 11 and 40 meV) in a semimetallic InAs/GaSb double heterojunction (40-nm InAs well) in CR saturation measurements. Minima occurred approximately at the simple MPR condition (for $m=1$ and 2): $m\omega_c=\omega_{\mathrm{LO}}$, $m=1,2,...$, and $\omega_{\mathrm{photon}}=\omega_c$. Here ω_c is the CR energy in the vicinity of the Fermi energy and ω_{LO} is the LO-phonon energy ($\sim 242\ \mathrm{cm}^{-1}$) in InAs. Analysis is complicated in this case by the fact that the sample is semimetallic (the valence band in GaSb is higher in energy than the conduction band in InAs) and has low mobility. In addition, the duration of the

laser pulses (8–15 psec) is almost comparable to the effective lifetime, so that non-steady-state analysis was required.

In the present study, to understand the energy relaxation mechanisms between electron LL's uncomplicated by the presence of holes, we have investigated the effective LL lifetime (extracted from an *n*-level rate equation model) at frequencies between 51 and 130 cm^{-1}, in a high mobility semiconducting $InAs/Al_{0.5}Ga_{0.5}Sb$ single quantum well. We have observed oscillations (greater than an order of magnitude) in an effective LL lifetime similar to those obtained by Vaughan *et al.*[16]; however, in this instance the minima are shifted to higher frequencies than given by the simple parabolic MPR condition for $m=2$ and $m=3$. We attribute these shifts to large nonparabolicity in the InAs conduction band as discussed below. We have also carried out saturation measurements on a ''semimetallic'' $InAs/Al_{0.1}Ga_{0.9}Sb$ single quantum-well structure at 124-cm^{-1} laser frequency to investigate the physical origins of two previously observed lines, i.e., the so-called *X* line, which has been attributed to an internal transition of stable excitons,[17] and electron CR.

II. EXPERIMENTS

Two samples, both with a single InAs (15 nm) quantum well, but having different $Al_xGa_{1-x}Sb$ barrier compositions ($x=0.5$ and $x=0.1$), were studied. Sample 1 ($x=0.5$) is semiconducting with an electron density and mobility of 6.1×10^{11} cm^{-2} and 2.2×10^5 cm^2/V s, respectively. Sample 2 ($x=0.1$) is ''semimetallic'' ($Al_{0.1}Ga_{0.9}Sb$ valence band overlaps the InAs conduction band by about 110 meV in the absence of confinement) with an electron density of 5.5×10^{11} cm^{-2} and mobility of 0.5×10^5 cm^2/V s. The saturation spectroscopy experiments were carried out with the UCSB free-electron laser (FEL) in conjunction with a 12-T superconducting magnet with the sample mounted on a cold finger at ~1.5 K in the Faraday configuration. The UCSB FEL provides peak intensities up to 40 kW/cm^2 (when focused) over the frequency range between 4 and 160 cm^{-1} with pulse width variable between 0.5 and 5 μsec at a repetition rate of approximately 1 Hz. Measurements were made under steady-state conditions as all the relevant lifetimes are much shorter (nsec or less) than the 3.2-μsec FEL pulsewidth used in these experiments. A small split-off reference signal was detected by a pyroelectric detector, and a 4.2-K germanium bolometer was used to detect the signal transmitted through the sample. A digital oscilloscope was used to average (over four FEL pulses) the ratio of the transmitted signal to the reference signal. Far infrared radiation was focused on the sample with mirror optics. FEL frequencies between 51 and 130 cm^{-1} were used in this study.

III. SEMICONDUCTING SAMPLE ($x=0.5$)

A. Results

A typical series of magnetotransmission spectra is shown in Fig. 1 for several laser intensities at 130 cm^{-1}. At low laser intensities, the CR absorption lines are quite strong (33% change in transmission for the linearly polarized FEL beam). As the FEL intensity (corrected for reflection) increases, the absorption clearly decreases, and the CR linewidth broadens while shifting to higher magnetic fields. At the highest intensity, the CR is almost completely saturated. Nearly complete saturation of CR was obtained at all the FEL frequencies used.

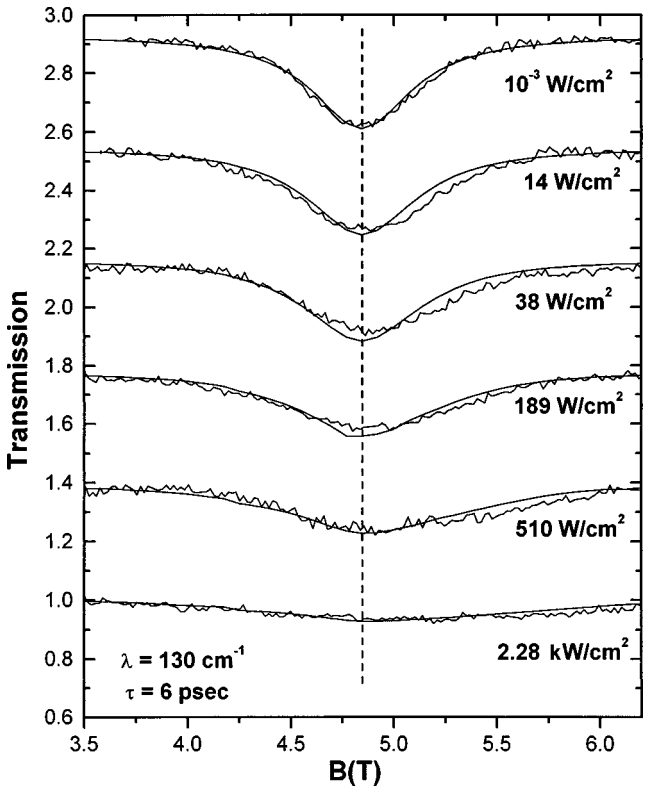

FIG. 1. The CR transmission spectra at 130 cm^{-1} at several laser intensities for sample 1. Solid smooth lines are the results of simulation using an *n*-level rate equation model for $\tau=6$ psec.

The peak absorption coefficient (α_{pk}) obtained from $\alpha_{pk}=-\ln[(2T/T_0)-1]$ is plotted as a function of intensity for several FEL frequencies in Fig. 2. Here T_0 is the transmitted intensity far from the resonant field, and T is the intensity transmitted at CR (transmission minimum), taking into account the fact that only half of the linearly polarized FEL

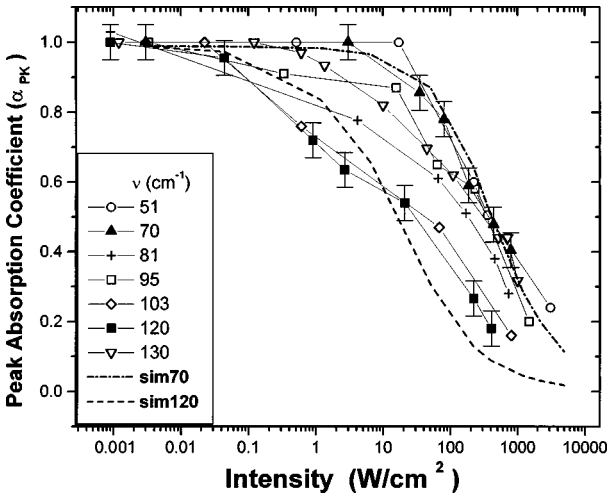

FIG. 2. Peak absorption coefficient vs intensity at several laser frequencies for sample 1. Dotted (Dashed) line is a fit for 70 (119) cm^{-1} laser line as described in the text. Solid lines are guides to the eyes.

beam satisfies the circular polarization selection rule for CR absorption. Several qualitative features can be noted from this plot. For the 119- and 103-cm^{-1} laser lines, α_{pk} decreases to half its low intensity value at approximately one order of magnitude lower intensity than for the other laser lines. Also, these two lines begin to saturate at a very low intensity, while complete saturation occurs at a high laser intensity (above 1 kW/cm^2). The low-frequency lines (51 and 70 cm^{-1}) do not show evidence of saturation until high intensities are reached, and then saturate rapidly. The 81-, 130-, and 95-cm^{-1} lines show onset of saturation at intermediate intensities, and reach complete saturation only at high intensities.

B. Model

The relaxation processes that compete in the carrier dynamics are (a) LO phonon emission,[12] a fast energy loss mechanism known to occur on a sub-psec time scale; (b) acoustic phonon scattering, for which energy loss occurs on a several hundred psec time scale; (c) ionized impurity scattering, an elastic thermalizing process that does not contribute to net energy loss of the electron gas and may occur on a psec time scale; and (d) electron-electron (e-e) scattering (Auger scattering), a very fast thermalizing process (subpsec) at low magnetic fields, which also does not contribute to net energy loss of the electron gas. At high fields Auger processes are less efficient in a system with strong nonparabolicity (unequal LL separation), because of the reduction in phase space that can satisfy energy conservation. In the phonon-emission processes, conservation of energy and momentum as well as the Pauli exclusion principle are strictly obeyed, and this dictates whether emission of LO phonons or acoustic phonons will be the dominant relaxation mechanism. The efficiency of these relaxation processes depends on magnetic field, temperature, and laser intensity. Due to the complex nature of the relaxation processes, we have made several simplifying assumptions to extract an effective LL lifetime ($\tau=1/\Gamma$) from an n-level rate equation model. We have considered nonradiative transitions with a relaxation rate Γ_n only between adjacent LL's neglecting spin splitting[18]; here Γ_n represents an average relaxation rate from the nth LL due to all possible relaxation processes. Moreover, the resonant nature of the LO-phonon emission is not directly incorporated in the model, but appears indirectly in the lifetime extracted from the model by fitting the experimental data. The fact that the relaxation rate between adjacent LL's increases with increasing LL index n is approximately taken into account by assuming $\Gamma_n=n\Gamma$, where Γ is an effective relaxation rate from $1\rightarrow 0$; this takes the leading (dipole) term into account in the interaction matrix element. For each Landau level $n\geqslant 1$, a rate equation accounting for stimulated absorption, stimulated emission, and nonradiative emission can be written as

$$dN_n/dt=\sigma_{n-1}IN_{n-1}S_n-\Gamma_nN_nS_{n-1}-\sigma_{n-1}IN_nS_{n-1}-\sigma_nIN_nS_{n+1}+\Gamma_{n+1}N_{n+1}S_n+\sigma_nIN_{n+1}S_n, \tag{1}$$

where I is the flux of incident photons, N_n is the carrier density of the nth LL, $\Gamma_n=1/\tau_n$ is the average relaxation rate from the nth LL, τ_n is the effective LL lifetime for the nth LL, $S_n=1-N_n/g$ is the fractional number of available empty states of the nth LL (g is the LL degeneracy including spin), and σ_n is the absorption cross section[6] for the nth LL (independent of laser intensity) given by

$$\sigma_n(B)=\frac{4\pi^2e^2\gamma_c|\langle n+1|\hat{\xi}\cdot\mathbf{P}|n\rangle|^2}{2\pi cr\omega_cm_n^{*2}[(\omega_n-\omega_c)^2+\gamma_c^2/4]}. \tag{2}$$

Here r is the index of refraction of the medium, m_n^* is the effective mass of electrons in the nth LL including nonparabolicity,[19] $\hat{\xi}$ is the polarization vector of the incident radiation, ω_c is the CR frequency, B is the magnetic field, ω_n is the energy spacing between the nth and $(n+1)$th LL at a magnetic field B, and γ_c is a phenomenological broadening constant, which represents the LL absorption line profile at low intensity. Since $|\langle n+1|\hat{\xi}\cdot\mathbf{P}|n\rangle|^2\propto n+1$,[9] Eq. (2) may be written as

$$\sigma_n(B)=\frac{A_n(B)(n+1)}{\omega_cm_n^{*2}[(\omega_n-\omega_c)^2+\gamma_c^2/4]}. \tag{3}$$

The constant of proportionality $A_n(B)$ in Eq. (3) is obtained by fitting the lowest intensity data. The absorption coefficient α is given by

$$\alpha(I,B)=\sum_n\ \sigma_n(B)[N_n(I,B)-N_{n+1}(I,B)]. \tag{4}$$

Since the total electron sheet density in the quantum well, N_{total}, is constant, we have the constraint

$$N_{total}=\sum_n\ N_n(I,B). \tag{5}$$

C. Comparison with experiments and discussion

The coupled rate equations [Eq. (1)] along with Eqs. (2)–(5) are solved numerically to obtain α_{pk} as a function of intensity at the resonant magnetic field (transmission minimum) under steady-state conditions ($dN_n/dt=0$) with only τ as an adjustable parameter. We find that ten LL's or more are significantly populated at high intensities. Examples of the results of this simulation for α_{pk} are shown in Fig. 2 for the 70 cm^{-1} (dotted line) and 119 cm^{-1} (dashed) laser lines; the fit is very good for the 70 cm^{-1} line but is much poorer for the 119-cm^{-1} line in a systematic way. In the latter case the fit *overestimates* the absorption at low and intermediate intensities but *underestimates* the absorption at high intensities. This systematic behavior is discussed further below. Lifetimes are extracted for all the laser frequencies with this procedure. The value of lifetime τ thus obtained at the resonant magnetic field can be used to simulate the CR transmission spectra at any laser intensity. Examples of these results are shown by smooth solid lines in Fig. 1 for the 130-cm^{-1} laser line. Though the simulation underestimates the absorption at higher fields for higher laser intensities, it reproduces reasonably well the general features of the transmission spectra (note that there is no *fitting* involved in this comparison). The line loses strength, broadens, and shifts to higher fields with increasing intensity. Thus, the absorption strength, the

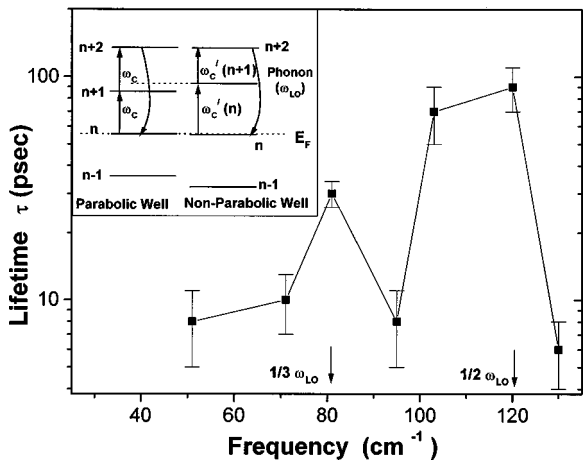

FIG. 3. The effective Landau-level lifetime from an n-level rate equation model is plotted as a function of frequency for sample 1. MPR conditions are shifted to higher frequencies $[\omega_c'(n)>\omega_c]$ for a nonparabolic well as shown in the inset.

shift, and the broadening of the line at high intensities can be explained reasonably well by the model.

The effective lifetime τ obtained from the model shows strong oscillations with frequency (greater than one order of magnitude) as shown in Fig. 3. When the MPR condition is satisfied, one expects large resonant enhancement of the scattering rate (minima in lifetime) due to LO-phonon emission from partially occupied LL's that lie $\hbar\omega_{\rm LO}$ above partially unoccupied LL's. Since the LO-phonon energy for InAs is approximately 242 $\rm cm^{-1}$, the MPR conditions for a simple parabolic InAs conduction band (equally spaced LL's) are satisfied at 121 $\rm cm^{-1}$ $(m=2)$ and 81 $\rm cm^{-1}$ $(m=3)$. In contrast, the present results show *minima* around 90–95 $\rm cm^{-1}$ and 130 $\rm cm^{-1}$, and *maxima* at approximately 80 and 110 $\rm cm^{-1}$.

This apparent disagreement is due to the large nonparabolicity in the InAs conduction band. Due to nonparabolicity, the energy spacing between adjacent LL's becomes smaller with increasing energy as shown in the inset of Fig. 3. The MPR condition $m=2$ for this situation will be satisfied when $\omega_c'(n+1)+\omega_c'(n)=\omega_{\rm LO}$, where the Fermi level is assumed to be in the nth LL at low laser intensities, rather than the simple parabolic condition $2\omega_c=\omega_{\rm LO}$. Since $\omega_c'(n+1)<\omega_{\rm LO}/2$ due to nonparabolicity, $\omega_c'(n)$ must be greater than $\omega_{\rm LO}/2$ for the MPR condition to be satisfied. Hence, the MPR conditions are satisfied at higher photon frequencies (higher resonant fields). A simple calculation of the nonparabolicity[19] predicts the MPR conditions to be satisfied around 127 $\rm cm^{-1}$ $(m=2)$ and 90 $\rm cm^{-1}$ $(m=3)$, in reasonable agreement with the experimental results.

The fact that the fits for the 103- and 119 $\rm cm^{-1}$ lines overestimate the peak absorption coefficient at intermediate intensities but underestimate the peak absorption coefficient at high intensities, shown in Fig. 2, is also related to nonparabolicity. The MPR condition $(m=2)$ between LL$(n+2)$ and LL(n) (see inset of Fig. 3) is not satisfied for these laser lines (as explained above) at the CR resonant field. Moreover, LL$(n+2)$ is only partially occupied at low and intermediate intensities. Relaxation from LL$(n+1)$ to LL$(n-1)$ is not allowed as LL$(n-1)$ is almost completely occupied at low and intermediate intensities. Hence, relaxation occurs mainly via emission of acoustic phonons a much less efficient process than LO-phonon emission. This accounts for the fact that CR begins to saturate at a low intensity for these lines. At high laser intensities LL$(n-1)$ becomes significantly *depopulated* while LL$(n+1)$ becomes significantly populated, thus relaxation from LL$(n+1)$ to LL$(n-1)$ becomes possible. As the energy spacing between LL(n) and LL$(n-1)$ is larger than the energy spacing between LL$(n+1)$ and LL(n) due to nonparabolicity, the MPR condition $(m=2)$ can be energetically satisfied between LL$(n+1)$ and LL$(n-1)$. Hence, relaxation occurs mainly by emission of LO phonons, thus making it harder to saturate CR at higher intensities. Since the resonant nature of the LO-phonon emission is not incorporated in the model, the simulation doesn't reproduce the experimental data well for the 103 and 119 $\rm cm^{-1}$ laser lines. This effect is much more pronounced for these lines as the *dominant* relaxation mechanism changes drastically from acoustic phonon emission at low or intermediate intensities to LO-phonon emission at high intensities. On the other hand the fits for the 51- and 70-$\rm cm^{-1}$ laser frequencies are good as the dominant relaxation mechanism (LO-phonon emission) remains the same at low as well as high intensities: at low laser frequencies nonparabolicity is much smaller, and it is easier to satisfy the MPR condition for the relatively broad LL's with small inter-LL spacings.

The fact that the line-shape simulation at 130 $\rm cm^{-1}$, shown in Fig. 1, *underestimates* the absorption for higher intensities at higher fields can be accounted for by a similar argument. At high laser intensities higher Landau levels are significantly populated. The MPR condition $(m=2)$ between a pair of these higher LL's is satisfied more precisely at higher fields for the 130-$\rm cm^{-1}$ frequency, since the spacing between LL's becomes smaller with increasing energy. This can result in a significant depopulation (population) of a higher (lower) LL at the MPR condition, leading to an increased absorption from the lower LL. Since the model does not incorporate this resonant process it underestimates the absorption at higher fields. Also, at a magnetic field significantly higher than the resonant magnetic field, it is possible to populate higher LL's at very high laser intensities due to the energy broadening of the LL's. When the energy spacing between a pair of higher LL's become resonant with the laser frequency at a higher magnetic field, due to nonparabolicity, there is an increased absorption. This not only shifts the resonant magnetic field up, but also asymmetrically broadens the CR absorption line to high fields at higher intensities.

The absolute values of the effective LL lifetime obtained in the present experiment are accurate to only a factor of 2–3, mainly due to inaccuracy in measuring FEL spot size on the sample; the relative accuracy is better than $\pm 15\%$ as the same setup has been used for all the laser lines. The dominant relaxation mechanism for 103- and 119-$\rm cm^{-1}$ laser lines is acoustic phonon emission, consistent with measured lifetimes of the order of 100 psec. For the 130- and 95-$\rm cm^{-1}$ laser lines the relaxation occurs mainly by LO-phonon emission, and hence the lifetimes are several psec. Since it is easier to satisfy the MPR condition at low magnetic fields as the inter LL spacings are small and the LLs are relatively broad, lifetimes of several psec are also reasonable for the

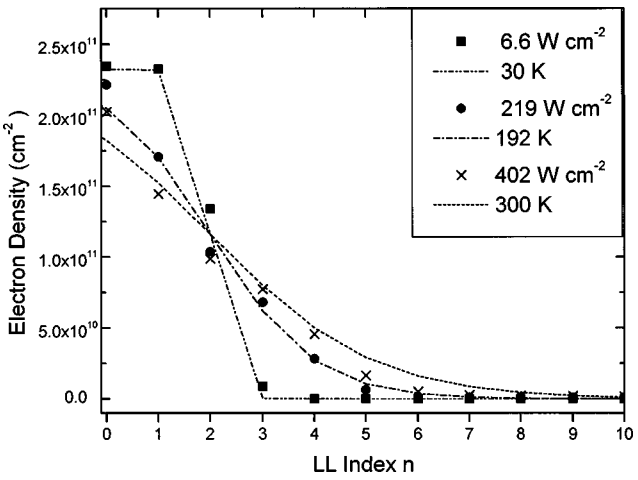

FIG. 4. The distribution of electrons among LL's at low, intermediate and high intensities for 130 cm^{-1} are shown from two different models for sample 1: the electron temperature model (lines) and the *n*-level rate equation model (scatters). These two models differ measurably at high intensities.

51- and 70-cm^{-1} laser frequencies. The values of the lifetimes extracted in the present study are in reasonable agreement with theoretical calculations in a magnetic field.[12,20]

In the usual electron temperature model, electron population in the higher LL's results from Auger processes (which permit the electron system to reach an internal equilibrium), and the distribution is given by a Fermi-Dirac function with a single effective electron temperature T_e. In saturation experiments, in the absence of Auger scattering, the electron population in the higher LLs is due to CR absorption from the broadened density of states of adjacent LLs at the resonant field; the distribution can be determined from an *n*-level rate equation model as above. The electron density as a function of LL index *n* is shown in Fig. 4 for the 130-cm^{-1} laser frequency for an electron temperature model and from the *n*-level rate-equation model. The overall agreement between these two models is reasonably good at low and intermediate intensities, but deviates measurably at high intensities. Therefore, it is clear that at high laser intensities the electron distribution among LL's cannot be described accurately by the electron temperature model. Nevertheless, the electron temperature model is a fair approximation. The electron temperatures at high intensities fall between 200 and 300 K, in reasonable agreement with theoretical calculations.[20]

IV. SEMIMETALLIC SAMPLE

We have also carried out saturation measurements on the ''semimetallic'' InAs/$Al_{0.1}Ga_{0.9}Sb$ single quantum-well structure at 124-cm^{-1} laser frequency in order to investigate the origins of two absorption lines previously reported.[17] For this structure the highest heavy-hole confinement subband in the $Al_{0.1}Ga_{0.9}Sb$ overlaps the lowest electron confinement subband in the InAs by ~60 meV at zero magnetic field. Results are shown in Fig. 5. The lower field line (the *X* line) has been attributed to an internal transition of spatially separated excitons[16] and the other line to electron CR. Recently, Chiang *et al.*,[21] based on their band-structure calculations, have reinterpreted these two lines as spin-split cyclotron

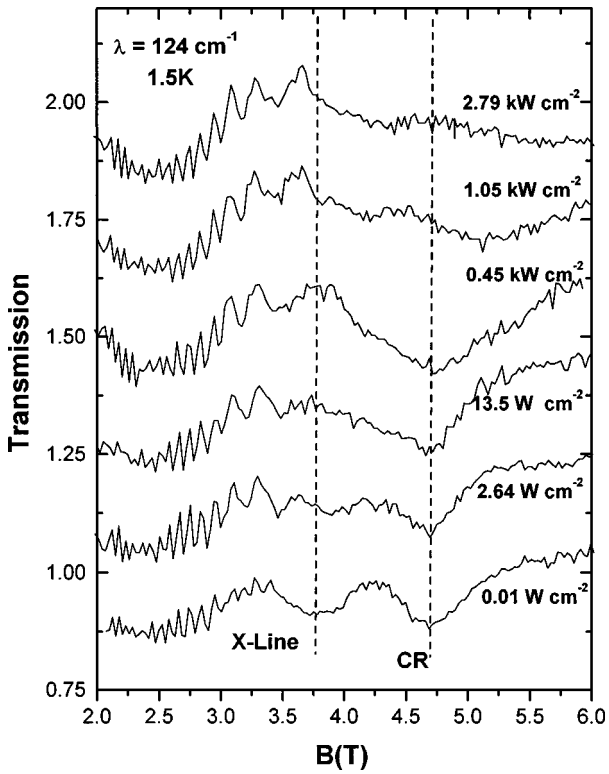

FIG. 5. Transmission spectra at 124 cm^{-1} at several laser intensities for sample 2. *X* line saturates at more than two orders of lower intensity than CR.

resonance transitions. The large separation (~3 meV) arising from the unique band structure,[22] which results from $\mathbf{k}\cdot\mathbf{p}$ coupling of the electron LL's in the InAs to the heavy-hole LL's in the $Al_{0.1}Ga_{0.9}Sb$.

In the present experiment, the *X* line saturates at a *much* lower laser intensity (more than two orders of magnitude) than CR, clearly indicating their different physical origin. The longer lifetime for the *x* line is consistent with the assignment of the *x* line to an internal transition of a stable exciton. Conversely, the CR line initially *gains strength* and then starts to saturate with further increase in laser intensity. The initial increase in CR strength is also consistent with this interpretation. Excitons can be impact ionized at high laser intensities, creating free electrons and holes, thus increasing the strength of CR. Another interesting feature in Fig. 5 is the presence of oscillations in transmission at low magnetic fields. These oscillations seem to be periodic in $1/B$, but the period does not correspond to the electron density. The origin of the oscillations is uncertain at present.

V. SUMMARY AND CONCLUSIONS

In conclusion, we have extracted effective LL lifetimes from CR saturation results using an *n*-level rate equation model. We have observed strong oscillations (greater than an order of magnitude) in the effective LL lifetime with frequency in a semiconducting InAs/$Al_{0.5}Ga_{0.5}Sb$ sample; minima occur at the modified MPR conditions for the nonparabolic InAs conduction band. The electron temperature model appears to be a fair approximation to the *n*-level rate equation model at low and intermediate intensities, but devi-

ates measurably at high intensities. For a ''semimetallic'' $InAs/Al_{0.1}Ga_{0.9}Sb$ sample, we have shown that the *X* line has a different physical origin than CR, and the assignment of the *X*-line to internal transition of excitons is consistent with our results.

ACKNOWLEDGMENT

This work was supported in part by the ONR-MFEL Program under Grant No. N000149710858.

[1] F. H. Julien, J.-M. Lourtioz, N. Herschkorn, D. Delacourt, J. P. Pocholle, M. Papuchon, R. Planel, and G. Le Roux, Appl. Phys. Lett. **53**, 116 (1988).

[2] M. C. Tatham, J. F. Ryan, and C. T. Foxon, Phys. Rev. Lett. **63**, 1637 (1989).

[3] G. R. Allan, A. Black, C. R. Pidgeon, E. Gornik, W. Seidenbusch, and P. Colter, Phys. Rev. B **31**, 3560 (1985).

[4] S. R. Ryu, G. Herold, J. Kono, M. Salib, B. D. McCombe, J. Kaminski, and S. J. Allen, Jr., Superlattices Microstruct. **21**, 2 (1997).

[5] K. Mitchell, A. Black, C. R. Pidgeon, G. R. Allan, M. F. Kimmitt, and E. Gornik, J. Phys. C **20**, 5217 (1987).

[6] M. Helm, E. Gornik, A. Black, G. R. Allan, C. R. Pidgeon, K. Mitchell, and G. Weiman, Physica B **134**, 323 (1985).

[7] I. Maran, W. Seidenbusch, E. Gornik, G. Weimann, and M. Shayegan, Semicond. Sci. Technol. **9**, 700 (1994).

[8] R. Ranganathan, J. Kaminski, W. J. Li, J.-P. Cheng, and B. D. McCombe, Proc. SPIE **1678**, 120 (1992).

[9] B. D. McCombe and R. J. Wagner, *Advances in Electronics and Electron Physics* (Academic Press, New York, 1975), pp. 1–78.

[10] Y. J. Yang, H. A. Nickel, B. D. McCombe, F. M. Peeters, J. M. Shi, G. Q. Hai, X.-G. Wu, T. J. Eustis, and W. Schaff, Phys. Rev. Lett. **79**, 3226 (1997).

[11] S. Das Sarma, J. K. Jain, and R. Jalabert, Phys. Rev. B **41**, 3561 (1990).

[12] P. Warmenbol, F. M. Peeters, X. Wu, and J. T. Devreese, Phys. Rev. B **40**, 6258 (1989).

[13] D. J. Barnes, R. J. Nicholas, F. M. Peeters, X.-G. Wu, J. T. Devreese, J. Singleton, C. J. G. M. Langerak, J. J. Harris, and C. T. Foxon, Phys. Rev. Lett. **66**, 794 (1991).

[14] M. A. Brummell, R. J. Nicholas, M. A. Hopkins, J. J. Harris, and C. T. Foxon, Phys. Rev. Lett. **58**, 77 (1987).

[15] V. L. Gurevich and Yu. A. Firsov, Zh. Eksp. Teor. Fiz. **40**, 199 (1961) [Sov. Phys. JETP **13**, 137 (1963)].

[16] T. A. Vaughan, R. J. Nicholas, C. J. G. M. Langerak, B. N. Murdin, C. R. Pidgeon, N. J. Mason, and P. J. Walker, Phys. Rev. B **53**, 16 481 (1996).

[17] J. Kono, B. D. McCombe, J.-P. Cheng, I. Lo, W. C. Mitchel, and C. E. Stutz, Phys. Rev. B **55**, 1617 (1997); J. Kono, B. D. McCombe, J.-P. Cheng, I. Lo, W. C. Mitchel, and C. E. Stutz, *ibid.* **50**, 12 242 (1994); J.-P. Cheng, J. Kono, B. D. McCombe, I. Lo, W. C. Mitchel, and C. E. Stutz, Phys. Rev. Lett. **74**, 450 (1995).

[18] A similar *n*-level rate equation model which took into account the spin splitting of the LL's was also explored. Results were not measurably different from those of the simple model neglecting spin splitting.

[19] D. J. Barnes, R. J. Nicholas, R. J. Warburton, N. J. Mason, P. J. Walker, and N. Miura, Phys. Rev. B **49**, 10 474 (1994).

[20] Xiaoguang Wu and F. M. Peeters, Phys. Rev. B **55**, 9333 (1997).

[21] Chiang *et al.*, Phys. Rev. Lett. **77**, 2053 (1996).

[22] A. Fasolino and M. Altarelli, Surf. Sci. **142**, 322 (1984).